Chinese Journal of Aeronautics, (2015), 28(6): 1629–1639

Chinese Society of Aeronautics and Astronautics
& Beihang University

Chinese Journal of Aeronautics

cja@buaa.edu.cn
www.sciencedirect.com

A hierarchical updating method for finite element model of airbag buffer system under landing impact

He Huan [a,b,*], Chen Zhe [a], He Cheng [c], Ni Lei [d], Chen Guoping [a,b]

[a] State Key Laboratory of Mechanics and Control of Mechanical Structures, Nanjing University of Aeronautics and Astronautics, Nanjing 210016, China
[b] Institute of Vibration Engineering Research, Nanjing University of Aeronautics and Astronautics, Nanjing 210016, China
[c] Research Institute of Pilotless Aircraft, Nanjing University of Aeronautics and Astronautics, Nanjing 210016, China
[d] China Aviation Industry General Aircraft Co. Ltd., Zhuhai 519040, China

Received 5 November 2014; revised 24 June 2015; accepted 24 August 2015
Available online 30 October 2015

KEYWORDS

Airbag;
Hierarchical model;
Impact;
Model updating;
Radial basis function

Abstract In this paper, we propose an impact finite element (FE) model for an airbag landing buffer system. First, an impact FE model has been formulated for a typical airbag landing buffer system. We use the independence of the structure FE model from the full impact FE model to develop a hierarchical updating scheme for the recovery module FE model and the airbag system FE model. Second, we define impact responses at key points to compare the computational and experimental results to resolve the inconsistency between the experimental data sampling frequency and experimental triggering. To determine the typical characteristics of the impact dynamics response of the airbag landing buffer system, we present the impact response confidence factors (IRCFs) to evaluate how consistent the computational and experiment results are. An error function is defined between the experimental and computational results at key points of the impact response (KPIR) to serve as a modified objective function. A radial basis function (RBF) is introduced to construct updating variables for a surrogate model for updating the objective function, thereby converting the FE model updating problem to a soluble optimization problem. Finally, the developed method has been validated using an experimental and computational study on the impact dynamics of a classic airbag landing buffer system.

1. Introduction

Research funding can be conserved and the research cycle can be shortened by constructing an accurate and reliable dynamics model for an airbag landing buffer. Simulation analysis could be used to study the impact dynamics of the airbag during the landing buffer process. However, for computational efficiency, the FE model needs to be simplified. For example, only the sealing effect of a fabric coating could be considered

* Corresponding author. Tel.: +86 25 84892142.
E-mail addresses: hehuan@nuaa.edu.cn (H. He), chenzhe617@163.com (Z. Chen), hechengary@nuaa.edu.cn (C. He), some0953@126.com (L. Ni), gpchen@nuaa.edu.cn (G. Chen).
Peer review under responsibility of Editorial Committee of CJA.

Production and hosting by Elsevier

http://dx.doi.org/10.1016/j.cja.2015.10.010

and its mechanical performance could be neglected. Another example would be to assume that the pressure inside the airbag is spatially uniform. These simplifications can produce errors between the computational and experimental results. The computational accuracy of the impact FE model of the airbag landing buffer system can be improved by model updating using experimental data.

Over the last thirty years, model updating technology has been developed in detail in the structure dynamics field. Numerous researchers have developed many finite element (FE) model updating methods for application in various fields in structure dynamics. The updating method, which is based on modal parameters, was the first of these methods to be developed and has had the widest application.[1–3] Göge adopted an updating method in which the modal frequency and vibrational sensitivity were used to update the finite element model for an Airbus A320 aircraft wing containing an engine pod, and frequency response function data were used to verify the reliability of the updating model.[4] Dascotte et al. studied the impact of updating results using a weight coefficient matrix selection an iterative scheme.[5] D'ambrogio and Fregolent showed that under certain conditions, modal parameter errors caused by experimental mode identification could be greater than errors resulting from an imprecise theoretical model.[6] Therefore, researchers have considered many modal parameter combinations as methods for updating the objective function. Thonon and Golinval used vibration-type related coefficients to provide supplementary information for the natural frequency in model updating.[7] Hanson et al. performed model updating using an anti-resonance frequency, which could have served as an effective supplement to the resonance frequency but relied largely on the updating variables that were selected and their values.[8] In addition, in recent years, developments in computer technology and uncertainty analysis theory have introduced new concepts into model updating. Goller et al. studied the uncertainty updating method within a Bayesian framework and applied this method to complex aero-structure model updating problems; the updating efficiency was greatly improved using a neural network.[9,10] The statistical characteristics of a response are very difficult to obtain when there is an insufficient number of supporting samples. Khodaparast et al. developed several non-probabilistic updating methods using surrogate model technology and validated these methods using experimental and numerical examples.[11,12]

Research on model updating problems considering nonlinear factors began relatively recently in the 1990s. Hemez and Doebling considered a system with multiple degrees of freedom and compared two updating schemes based on the least squares method and principal component decomposition for a transient time domain response; they also summarized model updating methods for nonlinear systems that are based on time domain signals and discussed key challenges.[13,14] Schultze and Hemez et al. used the response characteristics to extract and compress the data size and used a surrogate model to complete model updating for impact problems with uncertainty.[15] Hasselman et al. qualitatively and quantitatively studied the correlations, updating and uncertainty in a nonlinear model using principal component decomposition: the model was verified using numerical examples.[16] Li and Law developed a self-adaptive Tikhonov regularization method to update a nonlinear model in the presence of relatively high measured noise and compared the results with those obtained using a regular regularization model updating method.[17] Lenaerts et al. performed model updating on a nonlinear system using the proper orthogonal decomposition (POD) method and converted the model updating problem to an optimization problem by constructing a residual objective function using a proper orthogonal mode (POM) and experimental results.[18] He et al. investigated an updating problem for a structure dynamics model in a thermal environment using a radial basis surrogate model based on hierarchical concepts.[19]

Updating an impact FE model is a nonlinear problem that is relatively difficult to study. Experimental triggering, the sampling frequency, etc. usually result in the experimentally measured impact response not being synchronized with the computational impact response, which causes a significant disturbance in updating the impact dynamics model. In addition, an impact dynamics experiment typically has a long experimental cycle, and only a few experiments can be performed because of factors such as safety and cost. Therefore, a very limited amount of impact response experimental data can be obtained. If there are too many model updating variables (such as the parameter for the recovery module structural dynamics, the airbag internal pressure and the fabric thickness), this limited amount of impact response experimental data cannot satisfy the requirements of the updating scheme for the impact dynamics model.

In this study, we develop an updating method for an impact FE model of an airbag landing buffer system. First, the independence between the FE model for the recovery module structure and the airbag model are considered to develop a multi-step updating model. This multi-step updating scheme solves the problem of having a limited number of experimental samples and too many updating variables. In this study, the dynamics model for the recovery structure is accurately updated using a modal experiment. After completing the dynamics model updating for the recovery module structure, the updated dynamic parameters of the structure are used as known values to update the airbag parameters using the experimental data for the impact response. We use the multi-step updating method to reduce the maximum number of updating variables that are introduced into the final impact FE model, thereby reducing the experimental data required for the impact response experiment.

The measurement sensors used in the experiment have triggering level problems; thus, it is well-known that the experimental triggering time can be inconsistent with the initial time defined in the impact FE model. This inconsistency can lead to a discrepancy between the time at which the experimentally measured impact overloading peak occurs and the time at which the computed overloading peak occurs. Therefore, the impact overloading from the experimental and computational results cannot be compared directly at the same point in time. In this study, we use the impact peak time as a reference and the impact overloading response at equal time intervals on both sides of the impact peak time to construct an impact overloading response sequence to accurately resolve the time drift between the experimental and computational results. In addition, because the impact response data at the peak time and on both sides of the peak time can largely capture the shape of the impact overloading response curve, we use

the confidence factor of the impact response to evaluate the coherence between the computational and experimental impact overloading curves.

Finally, we use the impact response series at key time points to determine the error function between the computational and experiment results for the impact overloading. This error function then serves as a modified objective function. The radial basis function (RBF) method is used to update a surrogate model for the objective that depends on the updating variables. The updated results are obtained by optimizing the surrogate model.

2. Hierarchical FE model updating concept

An airbag landing buffer system has two parts: a recovery module and an airbag. During the overall landing buffer process, the system can be regarded as a local nonlinear system. In the dynamics substructure synthesis method,[20] the entire system can be divided into two substructures: a recovery module substructure and an airbag substructure. The finite element method can usually be used to discretize the airbag landing buffer system and develop equations for the impact dynamics of the system. We assume that the recovery module does not receive any external impact and neglect system damping. Then, the equations can be divided based on the degrees of freedom in the system. The dynamics equations for the recovery module substructure and the airbag substructure can be expressed in the following general form, respectively:

$$\boldsymbol{M}^{\mathrm{r}}\ddot{\boldsymbol{u}}^{\mathrm{r}}+\boldsymbol{K}^{\mathrm{r}}\boldsymbol{u}^{\mathrm{r}}=\begin{bmatrix}\boldsymbol{M}_{ii}^{\mathrm{r}} & \boldsymbol{M}_{ij}^{\mathrm{r}}\\ \boldsymbol{M}_{ji}^{\mathrm{r}} & \boldsymbol{M}_{jj}^{\mathrm{r}}\end{bmatrix}\begin{bmatrix}\ddot{\boldsymbol{u}}_i^{\mathrm{r}}\\ \ddot{\boldsymbol{u}}_j^{\mathrm{r}}\end{bmatrix}+\begin{bmatrix}\boldsymbol{K}_{ii}^{\mathrm{r}} & \boldsymbol{K}_{ij}^{\mathrm{r}}\\ \boldsymbol{K}_{ji}^{\mathrm{r}} & \boldsymbol{K}_{jj}^{\mathrm{r}}\end{bmatrix}\begin{bmatrix}\boldsymbol{u}_i^{\mathrm{r}}\\ \boldsymbol{u}_j^{\mathrm{r}}\end{bmatrix}=\begin{bmatrix}\boldsymbol{0}\\ \boldsymbol{F}_j^{\mathrm{r}}\end{bmatrix} \tag{1}$$

$$\boldsymbol{M}^{\mathrm{b}}\ddot{\boldsymbol{u}}^{\mathrm{b}}+\boldsymbol{K}^{\mathrm{b}}\boldsymbol{u}^{\mathrm{b}}=\begin{bmatrix}\boldsymbol{M}_{jj}^{\mathrm{b}} & \boldsymbol{M}_{jk}^{\mathrm{b}}\\ \boldsymbol{M}_{kj}^{\mathrm{b}} & \boldsymbol{M}_{kk}^{\mathrm{b}}\end{bmatrix}\begin{bmatrix}\ddot{\boldsymbol{u}}_j^{\mathrm{b}}\\ \ddot{\boldsymbol{u}}_k^{\mathrm{b}}\end{bmatrix}+\begin{bmatrix}\boldsymbol{K}_{jj}^{\mathrm{b}} & \boldsymbol{K}_{jk}^{\mathrm{b}}\\ \boldsymbol{K}_{kj}^{\mathrm{b}} & \boldsymbol{K}_{kk}^{\mathrm{b}}\end{bmatrix}\begin{bmatrix}\boldsymbol{u}_j^{\mathrm{b}}\\ \boldsymbol{u}_k^{\mathrm{b}}\end{bmatrix}=\begin{bmatrix}\boldsymbol{F}_j^{\mathrm{b}}\\ \boldsymbol{F}_k^{\mathrm{b}}\end{bmatrix} \tag{2}$$

where the superscript 'r' denotes the recovery module, and the superscript 'b' denotes the airbag. $\boldsymbol{M}^{\mathrm{r}}$ and $\boldsymbol{K}^{\mathrm{r}}$ represent the mass and stiffness matrices in the FE model of the recovery module, respectively, and $\boldsymbol{M}^{\mathrm{b}}$ and $\boldsymbol{K}^{\mathrm{b}}$ represent the mass and stiffness matrixes in the airbag FE model, respectively. The terms $\boldsymbol{u}_i^{\mathrm{r}}$ and $\boldsymbol{u}_j^{\mathrm{r}}$ represent the internal generalized displacement and the interfacial generalized displacement of the recovery module, respectively; i and j represent the internal and interfacial degrees of freedom, respectively, of the recovery module; $\boldsymbol{u}_j^{\mathrm{b}}$ and $\boldsymbol{u}_k^{\mathrm{b}}$ represent the interfacial and internal generalized displacements of the airbag, respectively; j and k represent the interfacial and internal degrees of freedom of the airbag, respectively. The terms $\boldsymbol{F}_j^{\mathrm{r}}$, $\boldsymbol{F}_j^{\mathrm{b}}$, and $\boldsymbol{F}_k^{\mathrm{b}}$ denote the interfacial force exerted on the recovery module, the interface force exerted on the airbag and the contact force exerted on the airbag.

In the substructure synthesis method,[20] the substructure must satisfy a generalized displacement continuity condition and an interfacial force compatibility condition.

$$\begin{cases}\boldsymbol{u}_j^{\mathrm{r}}=\boldsymbol{u}_j^{\mathrm{b}}\\ \boldsymbol{F}_j^{\mathrm{r}}+\boldsymbol{F}_j^{\mathrm{b}}=\boldsymbol{0}\end{cases} \tag{3}$$

Eqs. (1)–(3) can be used to derive the impact dynamics equation for the original system.

$$\begin{bmatrix}\boldsymbol{M}_{ii}^{\mathrm{r}} & \boldsymbol{M}_{ij}^{\mathrm{r}} & \boldsymbol{0}\\ \boldsymbol{M}_{ji}^{\mathrm{r}} & \boldsymbol{M}_{jj}^{\mathrm{r}}+\boldsymbol{M}_{jj}^{\mathrm{b}} & \boldsymbol{M}_{jk}^{\mathrm{b}}\\ \boldsymbol{0} & \boldsymbol{M}_{kj}^{\mathrm{b}} & \boldsymbol{M}_{kk}^{\mathrm{b}}\end{bmatrix}\begin{bmatrix}\ddot{\boldsymbol{u}}_i^{\mathrm{r}}\\ \ddot{\boldsymbol{u}}_j^{\mathrm{r}}\\ \ddot{\boldsymbol{u}}_k^{\mathrm{b}}\end{bmatrix}+\begin{bmatrix}\boldsymbol{K}_{ii}^{\mathrm{r}} & \boldsymbol{K}_{ij}^{\mathrm{r}} & \boldsymbol{0}\\ \boldsymbol{K}_{ji}^{\mathrm{r}} & \boldsymbol{K}_{jj}^{\mathrm{r}}+\boldsymbol{K}_{jj}^{\mathrm{b}} & \boldsymbol{K}_{jk}^{\mathrm{b}}\\ \boldsymbol{0} & \boldsymbol{K}_{kj}^{\mathrm{b}} & \boldsymbol{K}_{kk}^{\mathrm{b}}\end{bmatrix}\begin{bmatrix}\boldsymbol{u}_i^{\mathrm{r}}\\ \boldsymbol{u}_j^{\mathrm{r}}\\ \boldsymbol{u}_k^{\mathrm{b}}\end{bmatrix}=\begin{bmatrix}\boldsymbol{0}\\ \boldsymbol{0}\\ \boldsymbol{F}_k^{\mathrm{b}}\end{bmatrix} \tag{4}$$

It is obvious that Eq. (2) is typically a nonlinear equation, which exhibits the following characteristics: (a) there is a nonlinear relationship between the internal pressure and the compression of the airbag; and (b) the contact between the airbag and the landing surfaces is nonlinear.

Then, it is not difficult to show that $\boldsymbol{K}^{\mathrm{b}}$ depends on the current deformation $\boldsymbol{u}^{\mathrm{b}}$ and contact states of the airbag $\boldsymbol{\delta}$.

$$\boldsymbol{K}^{\mathrm{b}}=\boldsymbol{K}^{\mathrm{b}}(\boldsymbol{u}^{\mathrm{b}},\boldsymbol{\delta}) \tag{5}$$

In a typical design, the elastic deformation generated by the body structure of the recovery module during the airbag landing buffer process should satisfy the assumption of small deformations. Therefore, both $\boldsymbol{M}^{\mathrm{r}}$ and $\boldsymbol{K}^{\mathrm{r}}$ in Eq. (1) are constant matrices. This result shows that the dynamics FE model of the recovery module structure can still be described using a linear system; thus, the dynamic response of the system to the interfacial force $\boldsymbol{F}_j^{\mathrm{r}}$ can be computed using a mode superposition method.

The characteristics of the airbag landing recovery system in the landing buffer process are determined by performing a recovery module mode experiment. The recovery module model parameters are then updated such that the characteristics of the dynamics FE model for the recovery module structure matches those measured in the mode experiment. The updated recovery module FE model parameters are then used to formulate an impact FE model for the overall airbag landing buffer system. An impact dynamics experiment is then performed. These experimental results are in turn used to update the airbag model parameters.

3. RBF method

The RBF is the commonly used surrogate model technique in optimization, structural health monitoring and model updating. It is constructed by a series of basic functions which are symmetric and centered at each sampling point as one type of method for scattered multivariate data interpolation to replace the full finite element mathematical model. Usually, the sampling points are determined by experimental design methods (DOE), such as full factorial design (FFD) and central composite design (CCD). The idea of the surrogate model is shown in Fig. 1. In this section, we give a brief overview of RBF.

A generalized form of the RBF predictor for a system with n sampling points can be written based on the equation of the RBF, given in Eq. (6) as

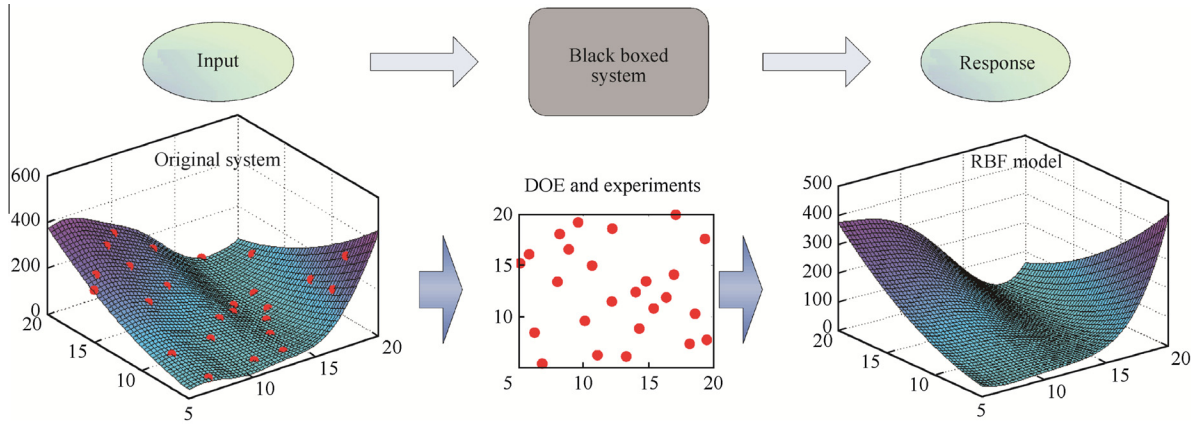

Fig. 1 Construction of surrogate model by RBF.

$$\bar{f}(\boldsymbol{x}) = \sum_{i=1}^{n} \lambda_i \phi(\|\boldsymbol{x} - \boldsymbol{x}_i\|) \tag{6}$$

where ϕ the basis function, and λ_i the weighted coefficient to be determined. $\|\boldsymbol{x} - \boldsymbol{x}_i\|$ is the Euler distance between an updating variable $\boldsymbol{x}$ and the ith sample point $\boldsymbol{x}_i$.

For convenience, we denote that $r = \|\boldsymbol{x} - \boldsymbol{x}_i\|$. Then, the most commonly used basis functions are listed as follows:

(a) The Gaussian distribution function $\phi(r) = \mathrm{e}^{-cr^2}$.
(b) The multi-quadric function $\phi(r) = \sqrt{r^2 + c^2}$.
(c) The inverse multi-quadric function $\phi(r) = \frac{1}{r^2 + c^2}$.

where c is the coefficient that can be determined by the cross validation method.

Substituting the function values at n sample points into Eq. (6) and letting $\bar{f}(\boldsymbol{x}_i) = f(\boldsymbol{x}_i)$ yields

$$f(\boldsymbol{x}_j) = \sum_{i=1}^{n} \lambda_i \phi(\|\boldsymbol{x}_j - \boldsymbol{x}_i\|) \quad j = 1, 2, \ldots, n \tag{7}$$

Eq. (7) can be rewritten in matrix form as

$$\boldsymbol{f} = \boldsymbol{A}\boldsymbol{\lambda} \tag{8}$$

where

$$\begin{cases} \boldsymbol{f} = [f(\boldsymbol{x}_1) \quad f(\boldsymbol{x}_2) \quad \cdots \quad f(\boldsymbol{x}_n)]^{\mathrm{T}} \\ \boldsymbol{\lambda} = [\lambda_1 \quad \lambda_2 \quad \cdots \quad \lambda_n]^{\mathrm{T}} \\ A_{ij} = \phi(\|\boldsymbol{x}_i - \boldsymbol{x}_j\|) \quad i, j = 1, 2, \cdots, n \end{cases} \tag{9}$$

Most of the basis functions used in RBF is strongly nonlinear functions. Thus, when the response values contain obviously linear components, it is difficult to obtain satisfactory results using the global approximation function model, which is constructed from a simple RBF. To solve this problem, Fang et al. combined classic response surface methodology (RSM) with RBF[21] to derive Eq. (10).

$$\bar{f}(\boldsymbol{x}) = \sum_{i=1}^{n} \lambda_i \phi(\|\boldsymbol{x} - \boldsymbol{x}_i\|) + \sum_{s=1}^{m} \beta_s q_s(\boldsymbol{x}) \tag{10}$$

where m is the order of the RSM model, $q_s(\boldsymbol{x})$ is a sth order polynomial, and β_s $(s = 1, 2, ..., m)$ represents the weight coefficients to be determined.

Introducing the orthogonal condition.

$$\sum_{i=1}^{n} \lambda_i q_s(\boldsymbol{x}_i) = 0 \quad s = 1, 2, ..., m \tag{11}$$

substitute Eq. (11) into Eq. (10) and combine the result with Eq. (10) to obtain the following matrix equation

$$\begin{bmatrix} \boldsymbol{A} & \boldsymbol{Q} \\ \boldsymbol{Q}^{\mathrm{T}} & \boldsymbol{0} \end{bmatrix} \begin{bmatrix} \boldsymbol{\lambda} \\ \boldsymbol{\beta} \end{bmatrix} = \begin{bmatrix} \boldsymbol{f} \\ \boldsymbol{0} \end{bmatrix} \tag{12}$$

where $Q_{is} = q_s(\boldsymbol{x}_i)$, $\boldsymbol{\beta} = [\beta_1 \quad \beta_2 \quad \cdots \quad \beta_m]^{\mathrm{T}}$.

Eq. (12) shows that the undetermined coefficients $\boldsymbol{\lambda}$ and $\boldsymbol{\beta}$ can be derived using a given actual $\boldsymbol{f}$ value. Then, the computed undetermined coefficients $\boldsymbol{\lambda}$ and $\boldsymbol{\beta}$ can be substituted into Eq. (10) to derive the approximate system response $\bar{f}(\boldsymbol{x})$.

4. Updating impact FE model

4.1. Impact response confidence factor (IRCF)

The primary characteristics of the impact response are the amplitude and the pulse width. In this study, key points in time corresponding to the peak and on both sides of the peak are selected. The consistency between the computational and experimental results is evaluated from the results at these key points.

Let us denote the actual measured impact overloading by $\boldsymbol{a}$, the time at which the experimentally measured impact overloading peak occurs by t_0 and the actual measured peak overloading by a_0. We consider equal time intervals Δt to extract the impact response overloading values at the overloading peak and on both sides of the peak. All of the impact responses at the $2n + 1$ time points are then used to construct the overloading sequence at the experimentally measured key points.

$$\boldsymbol{a}_{\mathrm{t}} = [a_{-n} \quad a_{-n+1} \quad \cdots \quad a_0 \quad \cdots \quad a_{n-1} \quad a_n]^{\mathrm{T}} \tag{13}$$

Let us denote the computed impact overloading by $\bar{\boldsymbol{a}}$ the time of the computational impact overloading peak as $\bar{t}_0$ and the computed peak overloading by $\bar{a}_0$. The computed impact overloading values at the overloading peak time and at $2n$ points on both sides of the peak (which results in a total of $2n + 1$ time points) can be similarly used to construct the impact overloading sequence at key time points.

$$\boldsymbol{a}_{\mathrm{c}} = [\bar{a}_{-n} \quad \bar{a}_{-n+1} \quad \cdots \quad \bar{a}_0 \quad \cdots \quad \bar{a}_{n-1} \quad \bar{a}_n]^{\mathrm{T}} \tag{14}$$

Usually, the experimental triggering time does not synchronize with the initial time of the computational model, i.e., $\bar{t}_0 \neq t_0$. However, Eqs. (13) and (14) show that the impact overloading sequence at key time points actually captures the shape and the characteristics of the impact response curve around the peak.

Then, the IRCF can be defined as

$$\mathrm{RAC} = \frac{\left|\boldsymbol{a}_{\mathrm{t}}^{\mathrm{T}}\boldsymbol{a}_{\mathrm{c}}\right|^2}{\left(\boldsymbol{a}_{\mathrm{t}}^{\mathrm{T}}\boldsymbol{a}_{\mathrm{t}}\right)\left(\boldsymbol{a}_{\mathrm{c}}^{\mathrm{T}}\mathbf{a}_{\mathrm{c}}\right)} \tag{15}$$

The RAC value is an indicator to verify the accuracy of the FE model. It is obvious that as the RAC value approaches 1.0, the computational results become more consistent with the experimental results, i.e., the impact FE model becomes more accurate.

4.2. Updating objective

Let us consider a total of l updating variables in the FE model, and denote the updated sample points obtained by combining l updating variables as follows:

$$\boldsymbol{x} = \begin{bmatrix} x^{(1)} & x^{(2)} & \dots & x^{(l)} \end{bmatrix}^{\mathrm{T}} \tag{16}$$

An impact FE model for the airbag landing buffer system can be formulated at any updating sample point $\boldsymbol{x}$. Dynamic computation is then used to obtain the impact overloading response and the impact overloading sequence $\boldsymbol{a}_{\mathrm{c}}(\boldsymbol{x})$ is constructed at key time points. The impact overloading sequence $\boldsymbol{a}_{\mathrm{t}}$ can be similarly obtained at key time points from the experimentally measured impact overloading.

Let us denote the error between the experimentally measured impact of the overloading sequence $\boldsymbol{a}_{\mathrm{t}}$ and the computed impact of the overloading sequence $\boldsymbol{a}_{\mathrm{c}}(\boldsymbol{x})$ at key points in time as follows:

$$\boldsymbol{\varepsilon} = \boldsymbol{a}_{\mathrm{t}} - \boldsymbol{a}_{\mathrm{c}}(\boldsymbol{x}) \tag{17}$$

We define the impact overloading sequence error function as

$$f(\boldsymbol{x}) = \sqrt{\frac{\boldsymbol{\varepsilon}^{\mathrm{T}}\boldsymbol{\varepsilon}}{2n+1}} \tag{18}$$

An error function $f(\boldsymbol{x}_s)$ can be obtained at any sampling point $\boldsymbol{x}_s = [x_s^{(1)}\ x_s^{(2)}\ \dots\ x_s^{(l)}]^{\mathrm{T}}$, for example. The actual updated sample point $\bar{\boldsymbol{x}}$ should be chosen to minimize the error function $f(\boldsymbol{x})$. Therefore, the updating problem can be converted to an optimization problem.

$$\begin{cases} \text{find} & \boldsymbol{x} \\ \min & f \\ \text{s.t.} & \boldsymbol{x}_{\mathrm{l}} \leqslant \boldsymbol{x} \leqslant \boldsymbol{x}_{\mathrm{u}} \end{cases} \tag{19}$$

where $\boldsymbol{x}_{\mathrm{l}}$ and $\boldsymbol{x}_{\mathrm{u}}$ are the upper and lower limits respectively.

The airbag landing buffer FE model is relatively complex; thus, the corresponding dynamics analysis involves nonlinear factors such as contact inequality constraints and large deformations, and an explicit function relating the model parameter $\boldsymbol{x}$ to the system impact response cannot be developed. That is, the model parameter $\boldsymbol{x}$ cannot be used to determine an explicit expression for $f(\boldsymbol{x})$, as shown in Eq. (18).

Thus, a nonlinear transient finite element analysis program is used to construct the updating variable sampling space $\boldsymbol{x}_1$, $\boldsymbol{x}_2, \dots, \boldsymbol{x}_l$ from which the impact overloading can be calculated at every sample point. After extracting the impact overloading sequence at the key time points, the RBF method is used to construct the surrogate model $\bar{f}$ using Eq. (18). This surrogate model then replaces the actual error function in Eq. (18) in the optimization analysis, as shown below:

$$\begin{cases} \text{find} & \boldsymbol{x} \\ \min & \bar{f} \\ \text{s.t.} & \boldsymbol{x}_{\mathrm{l}} \leqslant \boldsymbol{x} \leqslant \boldsymbol{x}_{\mathrm{u}} \end{cases} \tag{20}$$

Based on the discussion above, the following procedure is advised to update the flow for the impact FE model.

(a) Collect the experimental data for the impact response.
(b) Identify the time at which the impact response peak occurs. Then, select appropriate time intervals and a certain number of overloading data on both sides of the impact response peak. Construct an impact overloading sequence for the experimentally measured key points.
(c) Construct an updating variable sampling space $\boldsymbol{x}_1, \boldsymbol{x}_2, \dots, \boldsymbol{x}_l$: for any sample point $\boldsymbol{x}_i$, construct an FE model for the airbag landing buffer system, compute the impact overloading and extract the computational impact overloading sequence $\boldsymbol{a}_{\mathrm{c}}(\boldsymbol{x}_i)$ for the key points.
(d) Use Eqs. (17) and (18) to calculate $\boldsymbol{\varepsilon}(\boldsymbol{x}_i)$ and $f(\boldsymbol{x}_i)$ in sequence and generate the objective sequence $\boldsymbol{f} = [f(\boldsymbol{x}_1)\ f(\boldsymbol{x}_2) \dots f(\boldsymbol{x}_l)]^{\mathrm{T}}$.
(e) Select a basis function using Eq. (12) and determine $\boldsymbol{\lambda}$ and $\boldsymbol{\beta}$.
(f) Substitute $\boldsymbol{\lambda}$ and $\boldsymbol{\beta}$ into Eq. (10) to obtain a surrogate model $\bar{f}(\boldsymbol{x})$ for the error norm, as defined by Eq. (18).
(g) Optimize the surrogate model to obtain the updated results.

The detailed process of model updating of airbag buffer system is shown in Fig. 2.

5. Numerical example for updating an impact FE model for an airbag system

5.1. Experimental system

The experimental airbag landing buffer system consists of three airbags connected to each other at their bottoms and a recovery bracket, as shown in Fig. 3. The bracket was made of steel plate with a uniform thickness and a total mass of 3.0 kg. There were three circular steel plates at the bottom while an equilateral triangular steel plate on the top. Three steel buttress plates were used here to connect the top and bottom plates. The bolt holes were symmetrically distributed on the triangular plate to make it easy for installing the mass blocks and the acceleration sensors.

Fig. 4 shows the design for the impact dynamics experiment for the airbag landing buffer system. Before the experiment, the whole buffer system was lifted to a preset height and position using a bridge crane and a winch. Then, the control bomb

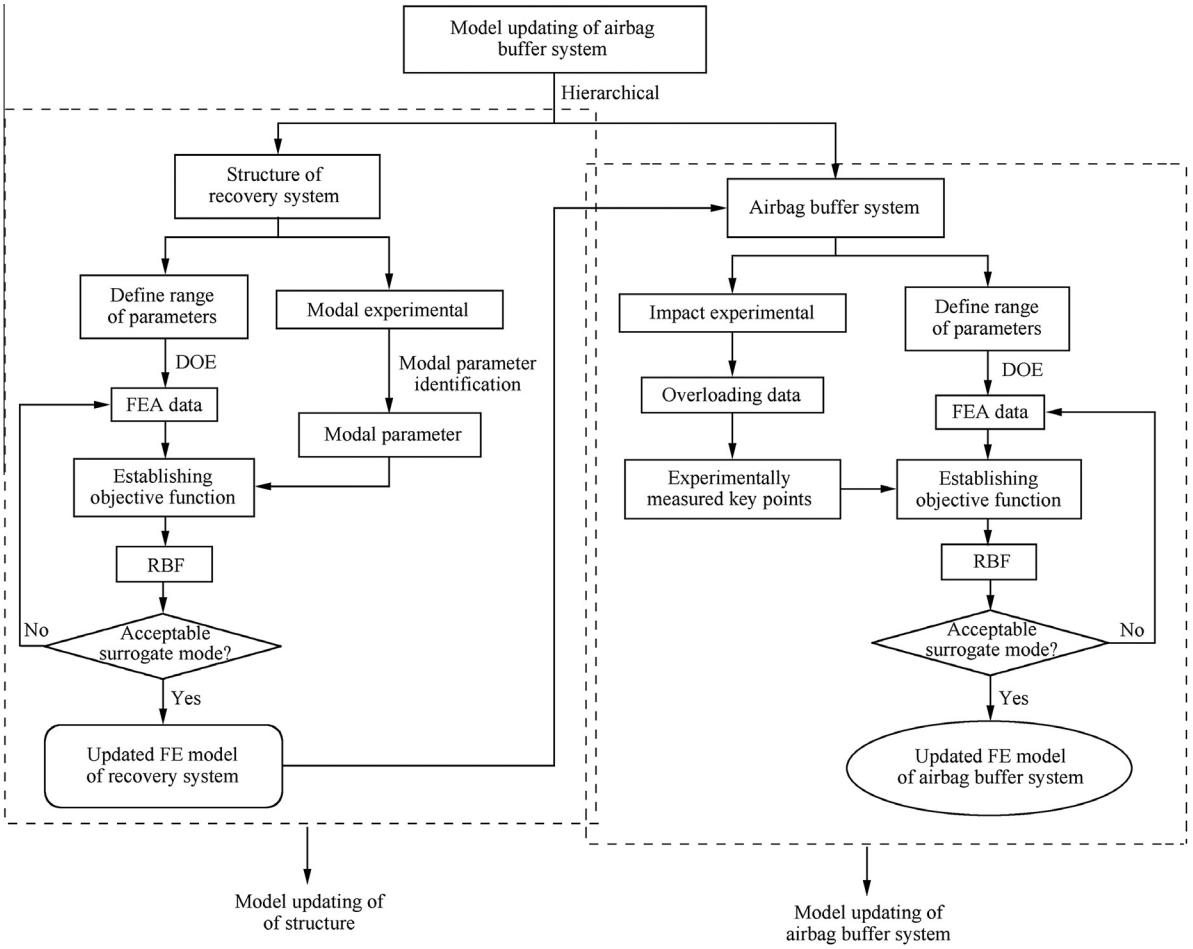

Fig. 2 Process of model updating of airbag buffer system.

Fig. 3 Experimental airbag buffer system.

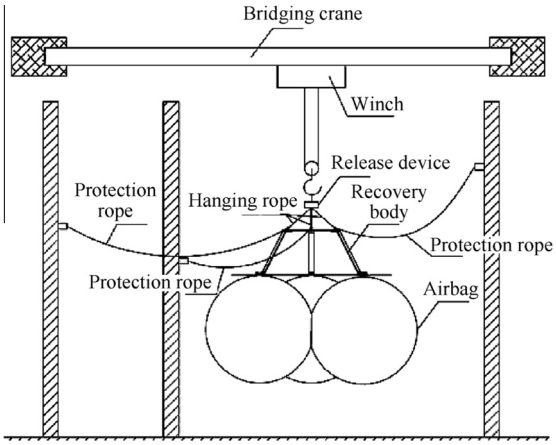

Fig. 4 Schematic of airbag landing buffer impact experiment.

hook was engaged to completely and freely drop the airbag landing system. A BW14108 acceleration sensor was used to measure the landing overloading of the recovery bracket, and a dynamic signal analyzer Agilent 35670 was used to collect and record the acceleration signals.

5.2. FE model of airbag system

An FE model based on the experimental apparatus was developed to describe the impact dynamics of the airbag landing buffer system. Shell elements were used to model the recovery bracket and 6-DOF (degrees of freedom) springs unit were used to simulate the equivalent stiffness of the screw connection between the steel plate and the circular plate and between the steel buttress plate and the triangular plate. Membrane elements were used to model the airbag fabric; cable elements were used to model the airbag external shrink rope. The air inside the airbag was assumed to be as the ideal gas and can

be described by using the ideal gas equation. The master–slave contact algorithm was used to simulate the interaction between the airbag model and the bottom of the recovery bracket model. The developed FE model for the airbag landing buffer system is shown in Fig. 5.

5.3. Updating FE model for structure of recovery bracket

Following the hierarchical updating scheme presented in Section 2, a mode experiment was used to update the FE model for the recovery bracket structure. In the experiment, three circular plates were fixed at the bottom, and a hammering method was used to measure the mode of the recovery bracket. I-DEAS was used to identify the natural frequency of the recovery bracket and the corresponding types of vibration.

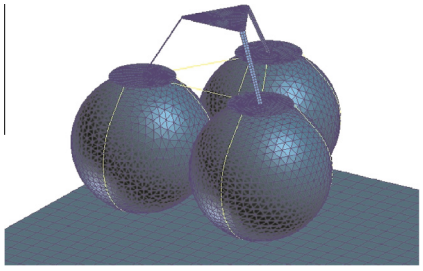

Fig. 5 FE model of airbag buffer system.

Preliminary simulations showed that the rotational stiffness of the 6-DOF spring unit (which was used to simulate the screw connection) was not sensitive to the modal analysis results. The numbers of updating variables were reduced by defining a screw rotational stiffness. The translational stiffness, the thickness, the elastic modulus and the density of the screw were selected as updating variables. Table 1 shows the updating variables in the parameter design space.

In Table 1, k_1, k_2 and k_3 denote the equivalent stiffness of the screw connection in the X, Y and Z directions.

An orthogonal experimental design was used, resulting in a total of 50 sampling points, as shown in Table 2. In which, p_1 to p_6 correspond to the normalized values of k_1, k_2, k_3, the thickness, the elastic modulus and the density of the recovery bracket in Table 1, respectively.

For every sample point in Table 2, MSC.Nastran was used to calculate the natural frequency of the recovery bracket. The sum of the absolute values of the weights for the residue between the first 4 orders of the measured natural frequencies for the recovery bracket and the corresponding computed natural frequencies are defined in Eq. (21).

Table 1 Design space for updating parameters for recovery bracket.

Item	k_1 (kN·m^{-1})	k_2 (kN·m^{-1})	k_3 (kN·m^{-1})	Thickness (mm)	Elastic modulus (GPa)	Density (kg·m^{-3})
Lower limit	300.00	300.00	300.00	2.9	190	7800
Upper limit	6000.0	6000.0	6000.0	3.1	220	8000

Table 2 Design matrix and normalized values of objective functions obtained from FE analysis of recovery bracket.

No.	p_1	p_2	p_3	p_4	p_5	p_6	E	No.	p_1	p_2	p_3	p_4	p_5	p_6	E
1	−1.0	−1.0	−1.0	−1.0	−1.0	−1.0	0.2380	26	1.0	1.0	1.0	1.0	1.0	1.0	0.5709
2	−1.0	−0.5	−0.5	−0.5	−0.5	−0.5	0.1149	27	1.0	0.5	0.5	0.5	0.5	0.5	0.4655
3	−1.0	0	0	0	0	0	0.1688	28	1.0	0	0	0	0	0	0.3510
4	−1.0	0.5	0.5	0.5	0.5	0.5	0.2226	29	1.0	−0.5	−0.5	−0.5	−0.5	−0.5	0.2746
5	−1.0	1.0	1.0	1.0	1.0	1.0	0.2858	30	1.0	−1.0	−1.0	−1.0	−1.0	−1.0	0.1280
6	−0.5	−1.0	−0.5	0	0.5	1.0	0.1629	31	0.5	1.0	0.5	0	−0.5	−1.0	0.3249
7	−0.5	−0.5	0	0.5	1.0	−1.0	0.2689	32	0.5	0.5	0	−0.5	−1.0	1.0	0.2541
8	−0.5	0	0.5	1.0	−1.0	−0.5	0.1283	33	0.5	0	−0.5	−1.0	1.0	0.5	0.3416
9	−0.5	0.5	1.0	−1.0	−0.5	0	0.1240	34	0.5	−0.5	−1.0	1.0	0.5	0	0.2602
10	−0.5	1.0	−1.0	−0.5	0	0.5	0.0940	35	0.5	−1.0	1.0	0.5	0	−0.5	0.3653
11	0	−1.0	0	1.0	−0.5	0.5	0.2615	36	0	1.0	0	−1.0	0.5	−0.5	0.2918
12	0	−0.5	0.5	−1.0	0	1.0	0.2585	37	0	0.5	−0.5	1.0	0	−1.0	0.3331
13	0	0	1.0	−0.5	0.5	−1.0	0.3511	38	0	0	−1.0	0.5	−0.5	1.0	0.1679
14	0	0.5	−1.0	0	1.0	−0.5	0.2292	39	0	−0.5	1.0	0	−1.0	0.5	0.2438
15	0	1.0	−0.5	0.5	−1.0	0	0.2381	40	0	−1.0	0.5	−0.5	1.0	0	0.3293
16	0.5	−1.0	0.5	−0.5	1.0	0	0.3851	41	−0.5	1.0	−0.5	0.5	−1.0	0	0.1198
17	0.5	−0.5	1.0	0	−1.0	0.5	0.2833	42	−0.5	0.5	−1.0	0	1.0	−0.5	0.1619
18	0.5	0	−1.0	0.5	−0.5	1.0	0.1896	43	−0.5	0	1.0	−0.5	0.5	−1.0	0.1987
19	0.5	0.5	−0.5	1.0	0	−1.0	0.3813	44	−0.5	−0.5	0.5	−1.0	0	1.0	0.1276
20	0.5	1.0	0	−1.0	0.5	−0.5	0.3315	45	−0.5	−1.0	0	1.0	−0.5	0.5	0.1348
21	1.0	−1.0	1.0	0.5	0	−0.5	0.3885	46	−1.0	1.0	−1.0	−0.5	0	0.5	0.1357
22	1.0	−0.5	−1.0	1.0	0.5	0	0.2711	47	−1.0	0.5	1.0	−1.0	−0.5	0	0.0629
23	1.0	0	−0.5	−1.0	1.0	0.5	0.3545	48	−1.0	0	0.5	1.0	−1.0	−0.5	0.1365
24	1.0	0.5	0	−0.5	−1.0	1.0	0.2634	49	−1.0	−0.5	0	0.5	1.0	−1.0	0.2648
25	1.0	1.0	0.5	0	−0.5	−1.0	0.3407	50	−1.0	−1.0	−0.5	0	0.5	1.0	0.2028

Table 3 Updated results for recovery bracket.

Item	k_1 (kN·m^{-1})	k_2 (kN·m^{-1})	k_3 (kN·m^{-1})	Thickness (mm)	Elastic modulus (GPa)	Density (kg·m^{-3})
Updated results	5760	4230	3590	2.90	204	7890

$$E = \sum_{i=1}^{4} \text{abs}(\bar{\omega}_i - \omega_i(\boldsymbol{p}))w_i \tag{21}$$

In Eq. (21), $\bar{\omega}_i$ is the actual measured ith order natural frequency, $\omega_i(\boldsymbol{p})$ is the ith natural frequency that was computed using an FE model for the recovery bracket structure based on the sample points $\boldsymbol{p}$, where $\boldsymbol{p} = [p_1 p_2 \ldots p_6]^{\mathrm{T}}$. The weight coefficients are denoted by w_i, where

$$\sum_{i=1}^{4} w_i = 1 \tag{22}$$

The actual updated sample points $\bar{\boldsymbol{p}}$ should minimize Eq. (21), i.e., the updating problem for the FE model of the recovery bracket structure is converted into an optimization problem:

$$\begin{cases} \text{find} & \boldsymbol{p} \\ \min & E \\ \text{s.}t. & \boldsymbol{p}_{\mathrm{l}} \leqslant \boldsymbol{p} \leqslant \boldsymbol{p}_{\mathrm{u}} \end{cases} \tag{23}$$

Table 2 shows the values of E that was derived using various sample points. The surrogate model for E was constructed using Eqs. (10) and (12) in which the inverse multi-quadric function is chosen to be the RBF basis, and a genetic algorithm was then used to obtain the optimal solution. The choice of the weight coefficients can directly impact the updating results. To ensure that each modal component contributed to the objective function as evenly as possible, $w_i = 1/\omega_i$ was selected as the weight coefficient for various orders of the modal coefficients.[22] In this study, our objective was to develop an updating method for an impact FE model of an airbag landing buffer system; thus, developing an optimization algorithm was outside the scope of this study and only the updated results are shown in Table 3.

Table 4 shows that the computational results obtained by updating the FE model were reasonably consistent with the experimentally measured results. To verify the computational accuracy of the updated FE model, a recovery free-free mode experiment was performed. The results for the experimentally measured first 7 orders of natural frequencies and the computed natural frequency for the recovery bracket are compared in Table 5.

Table 4 Comparison for first 4 orders of natural frequencies between experimentally measured results and FE results for recovery bracket.

Mode order	Natural frequency (Hz)		Error (%)	MAC
	Experiment	FEM		
1	37.60	37.90	0.80	0.96
2	105.80	103.60	2.08	0.97
3	181.00	185.90	2.71	0.96
4	193.30	200.80	3.88	0.98

Table 5 shows that the errors for the first 7 orders of natural frequencies between the experimental and computational results for the recovery bracket were all less than 5%. It can be observed from Tables 4 and 5 that all of the modal assurance criterion (MAC) values are close to 1.0, which means the updated results for the FE model of the recovery bracket were reliable and the FE model was used for a follow-up dynamics model for the landing buffer.

5.4. Updating FE model of airbag system

The experimental plan illustrated in Fig. 4 was used in an impact dynamics experiment for the airbag landing buffer system. The airbag system was lifted up to 1.0 m above ground. Using the free release method, the contact velocity between airbag and ground was found to be 4.43 m/s. The system had a total mass of 5.9 kg. One key time point was extracted for every 1 ms interval on both sides of the experimentally obtained peak for the impact overloading. The impact overloading peak value was used to construct an impact overloading sequence $\boldsymbol{a}_{\mathrm{t}}$, which was composed of 33 key points.

The airbag internal pressure and the equivalent elastic modulus of the airbag fabric were chosen as updating variables; the design space is shown in Table 6.

The updated variables were normalized, resulting in a full factorial experimental design with two factors and 7 levels, for a total of 49 sample points. MSC. Dytran was used to compute the impact overload for the airbag landing buffer system for the FE model at each sample point $\boldsymbol{x}_i$. The impact overloading sequence $\boldsymbol{a}_{\mathrm{c}}(\boldsymbol{x}_i)$ was similarly constructed. The error function values $f(\boldsymbol{x}_i)$ at every sample point (which were calculated based on Eq. (18), the inverse multi-quadric function is applied to forming the surrogate model as what we have done in Section 5.3) are shown in Table 7.

Then, Eqs. (10) and (12) was used to construct a surrogate model for the error function $\bar{f}(\boldsymbol{x})$, as shown in Fig. 6.

Table 5 Comparison for first 7 orders of natural frequencies between experimentally measured results and FE results for recovery bracket (free-free mode).

Mode order	Natural frequency (Hz)		Error (%)	MAC
	Experiment	FEM		
1	25.90	25.03	3.36	0.95
2	32.83	32.94	0.34	0.97
3	42.13	43.81	3.99	0.96
4	47.45	45.70	3.69	0.98
5	57.73	60.07	4.05	0.95
6	72.93	71.08	2.54	0.96
7	108.30	103.20	4.71	0.94

Table 6 Updating parameter design space for airbag model.

Item	Airbag internal pressure (kPa)	Fabric equivalent elastic modulus (MPa)
Lower limit	101.0	300.0
Upper limit	105.0	500.0

Table 7 Experimental design matrix and normalized values of error functions (used as objective functions) obtained from FE analysis of impact model for airbag buffer system.

No.	x_1	x_2	f	No.	x_1	x_2	f
1	−1.00	−1.00	1.777	26	0	0.33	1.562
2	−1.00	−0.67	2.881	27	0	0.67	1.505
3	−1.00	−0.33	3.070	28	0	1.00	2.111
4	−1.00	0	3.903	29	0.33	−1.00	3.244
5	−1.00	0.33	2.603	30	0.33	−0.67	3.029
6	−1.00	0.67	3.191	31	0.33	−0.33	1.329
7	−1.00	1.00	3.271	32	0.33	0	1.873
8	−0.67	−1.00	3.323	33	0.33	0.33	1.429
9	−0.67	−0.67	2.564	34	0.33	0.67	2.892
10	−0.67	−0.33	3.911	35	0.33	1.00	3.813
11	−0.67	0	2.555	36	0.67	−1.00	3.107
12	−0.67	0.33	2.774	37	0.67	−0.67	3.248
13	−0.67	0.67	1.823	38	0.67	−0.33	2.737
14	−0.67	1.00	2.054	39	0.67	0	1.400
15	−0.33	−1.00	2.856	40	0.67	0.33	1.191
16	−0.33	−0.67	3.956	41	0.67	0.67	2.939
17	−0.33	−0.33	2.088	42	0.67	1.00	3.457
18	−0.33	0	2.119	43	1.00	−1.00	3.311
19	−0.33	0.33	1.899	44	1.00	−0.67	3.150
20	−0.33	0.67	2.050	45	1.00	−0.33	5.052
21	−0.33	1.00	2.321	46	1.00	0	1.501
22	0	−1.00	3.312	47	1.00	0.33	5.597
23	0	−0.67	1.746	48	1.00	0.6667	2.448
24	0	−0.33	1.300	49	1.00	1.00	2.705
25	0	0	1.591				

A genetic algorithm was similarly used to optimize the surrogate model. The updated results for the parameters are shown in Table 8.

The impact FE model for the airbag landing buffer system was developed using the updated results and the impact overloading response was computed. The computed and experimental results are compared to each other in Table 9. Fig. 7 compares the computed and experimentally measured impact overloading curves to each other.

Table 9 shows that the error between the impact overloading peak value obtained from the updated FE model and the experiment measurements is only 0.37%. In Fig. 7, the computed impact overloading curve is very consistent with the experimentally measured curve. Eq. (15) was used to calculate that the IRCF value is 0.9985, indicating that the impact response confidence factor approaches 1.0. This result demonstrates a satisfactory updating accuracy for the updating method for the impact FE model that was developed for the airbag landing buffer system.

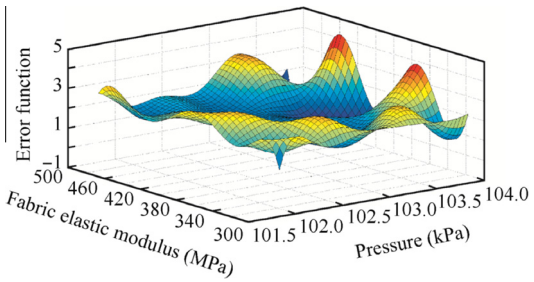

Fig. 6 Surrogate model for error function.

Table 8 Updated results for airbag FE model.

Item	Airbag internal pressure (kPa)	Fabric equivalent elastic modulus (MPa)
Value	103.403	427.8

Table 9 Comparison between peak overloading obtained from updated FE model and impact experiment results.

Item	Overloading peak (g)		Error (%)
	Experiment	FEM	
Value	24.49	24.58	0.37

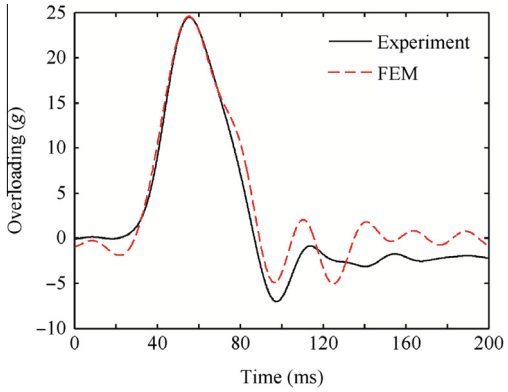

Fig. 7 Comparison of overloading obtained from updated FE model and impact experiment results.

To verify the prediction accuracy of the impact FE model of the airbag buffer system after updating, a 1.0 kg counterweight was added to the top recovery bracket of the airbag, resulting in a total system mass of 6.9 kg, while the contact velocity between the airbag and the ground remained at 4.43 m/s. A simulation was performed for this experimental configuration using an impact FE model for the updated airbag landing buffer system. The computed and experimentally measured results for the maximum impact overloading are compared to each other in Table 10.

Table 10 shows that using the updated FE model to simulate the landing impact process for the new experimental

Table 10 Comparison between peak overloading obtained from updated FE model and impact validation experiment.

Item	Overloading peak (*g*)		Error (%)
	Experiment	FEM	
Value	22.57	22.92	1.55

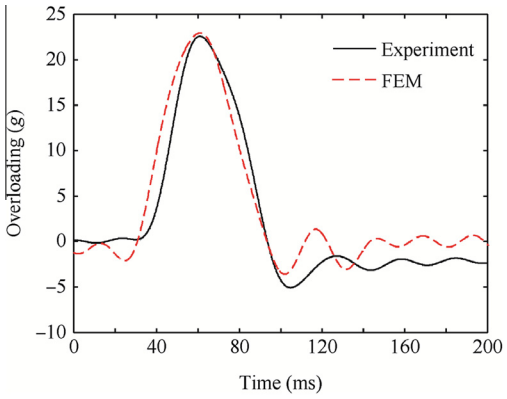

Fig. 8 Comparison between overloading obtained from updated FE model and impact validation experiment results.

configuration results in an error of 1.55% between the computed and experimentally measured overloading peak values.

Fig. 8 shows that the computed and experimentally measured impact overloading curves are consistent with each other. The IRCF value is 0.9908, which is still near 1.0. This result demonstrates good prediction accuracy of the updated FE model.

6. Conclusions

(1) In this study, a hierarchical updating scheme was combined with an RBF method to construct a surrogate model for the residue between the computational and experimental results for an impact response. In addition, optimization analysis was used to update an impact FE model for an airbag landing buffer system. Numerical examples were used to show that the method developed in this study could produce highly accurate impact FE models for an airbag landing buffer system.

(2) The results of this study also show that residues could be constructed between the computed and experimental results for the impact response by selecting impact response data at key points at the peak and on both sides of the peak, thereby effectively resolving the discrepancy between the sampling frequency and the experimental triggering.

(3) The methods developed in this study can be generalized to solve general updating problems for impact FE models.

Acknowledgements

This paper was co-supported by the National Natural Science Foundation of China (No. 11472132), the Fundamental Research Funds for Central Universities in China (No. NS2014002), the Research Fund of State Key Laboratory of Mechanics and Control of Mechanical Structures (Nanjing University of Aeronautics and Astronautics) (No. 0113Y01) and the Priority Academic Program Development (PAPD) of Jiangsu Higher Education Institutions in China.

References

1. Chen JC, Garba JA. Analytical model improvement using modal test results. *AIAA J* 1980;**18**(6):684–90.
2. Göge D, Link M. Results obtained by minimizing natural frequency and mode shape errors of a beam model. *Mech Syst Signal Process* 2003;**17**(1):21–7.
3. Chakraborty S, Sen A. Adaptive response surface based efficient finite element model updating. *Finite Elem Anal Des* 2014;**80**: 33–40.
4. Göge D. Automatic updating of large aircraft models using experimental data from ground vibration testing. *Aerosp Sci Technol* 2003;**7**(1):33–45.
5. Dascotte E, Strobbe J, Hua H. Sensitivity-based model updating using multiple types of simultaneous state variables. *Proceedings of the 13th International Modal Analysis Conference*; 1995 February 13–16; Nashville, TN. Bethel, CT: Society for Experimental Mechanics; 1995. p. 1113–6.
6. D'ambrogio W, Fregolent A. Results obtained by minimising natural frequency and antiresonance errors of a beam model. *Mech Syst Signal Process* 2003;**17**(1):29–37.
7. Thonon C, Golinval JC. Results obtained by minimising natural frequency and MAC-value errors of a beam model. *Mech Syst Signal Process* 2003;**17**(1):65–72.
8. Hanson D, Waters TP, Thompson DJ, Randall RB, Ford RAJ. The role of anti-resonance frequencies from operational mode analysis in finite element model updating. *Mech Syst Signal Process* 2007;**21**(1):74–97.
9. Goller B, Schueller GI. Investigation of model uncertainties in Bayesian structural model updating. *J Sound Vib* 2011;**330** (25):6122–36.
10. Goller B, Broggi M, Calvi A, Schueller GI. A stochastic model updating technique for complex aerospace structures. *Finite Elem Anal Des* 2011;**47**(7):739–52.
11. Khodaparast HH, Mottershead JE, Badcock KJ. Propagation of structural uncertainty to linear aeroelastic stability. *Comput Struct* 2010;**88**(3–4):223–36.
12. Marques S, Badcock KJ, Khodaparast HH, Mottershead JE. Transonic aeroelastic stability predictions under the influence of structural variability. *J Aircraft* 2010;**47**(4):1229–39.
13. Hemez FM, Doebling SW. Test-analysis correlation and finite element model updating for nonlinear, transient dynamics. *Proceedings of the 17th International Modal Analysis Conference;* 1999 February 8–11; Kissimmee, FL. Bethel, CT: Society for Experimental Mechanics; 1999. p. 1501–10.
14. Hemez FM, Doebling SW. Review and assessment of model updating for non-linear, transient dynamics. *Mech Syst Signal Process* 2001;**15**(1):45–74.
15. Schultze JF, Hemez FM, Doebling SW, Sohn H. Statistical based non-linear model updating using feature extraction. *Proceedings of IMAC-XIX, the 19th international modal analysis conference*; 2001 February 5–8; Kissimmee, FL. Bethel, CT: Society for Experimental Mechanics; 2001. p. 18–26.
16. Hasselman TK, Anderson MC, Wenshui G. Principal components analysis for nonlinear model, correlation, updating and uncertainty evaluation. *Proceedings of the 16th international modal analysis conference*; 1998 February 2–5; Santa Barbara, CA. Bethel, CT: Society for Experimental Mechanics; 1998. p. 664–51.

17. Li XY, Law SS. Adaptive Tikhonov regularization for damage detection based on nonlinear model updating. *Mech Syst Signal Process* 2010;**24**(6):1646–64.
18. Lenaerts V, Kerschen G, Golinval JC. Proper orthogonal decomposition for model updating of non-linear mechanical systems. *Mech Syst Signal Process* 2001;**15**(1):31–43.
19. He C, Chen GP, He H, Sun RJ. Model updating of a dynamic system in a high-temperature environment based on a hierarchical method. *Finite Elem Anal Des* 2013;**77**:59–68.
20. He H, Wang T, Chen GP, Sun D, Sun R. A real decoupled method and free interface component mode synthesis methods for generally damped systems. *J Sound Vib* 2014;**333**(2):584–603.
21. Fang H, Rais-Rohani M, Liu Z, Horstemeyer MF. A comparative study of metamodeling methods for multiobjective crashworthiness optimization. *Comput Struct* 2005;**83**(25–26):2121–36.
22. Mottershead JE, Link M, Friswell M. The sensitivity method in finite element model updating: a tutorial. *Mech Syst Signal Process* 2011;**25**(7):2275–96.

He Huan is an associate professor at State Key Laboratory of Mechanics and Control of Mechanical Structures, Nanjing University of Aeronautics and Astronautics. He received the B.S. degree in aircraft design from this university in 2001, then received the M.S. and Ph.D. degrees in engineering mechanics from the same university in 2004 and 2008 respectively. His main research interests are structural dynamics and finite element analysis.

Chen Zhe is a Ph.D. candidate at State Key Laboratory of Mechanics and Control of Mechanical Structures, Nanjing University of Aeronautics and Astronautics. She received the B.S. degree from Changsha University of Science and Technology in 2008. Her current researches focus on structural dynamic and model updating technique.

He Cheng is an aircraft engineer at Research Institute of Pilotless Aircraft, Nanjing University of Aeronautics and Astronautics. He received the Ph.D. degree from this university in 2014. His current research interests are unmanned aerial vehicles launching and recovery techniques.

Ni Lei is an aircraft engineer at China Aviation Industry General Aircraft Co. Ltd. He received his B.S. degree from Northwestern Polytechnical University in 2007, then he received the M.S. degree from Nanjing University of Aeronautics and Astronautics in 2010. His major research works are aircraft design and finite element analysis.

Chen Guoping is a professor and Ph.D. supervisor at Institute of Vibration Engineering Research, Nanjing University of Aeronautics and Astronautics. He received his B.S. and M.S. degrees from Zhejiang University in 1982 and 1984 respectively, then he received the Ph.D. degree from Nanjing University of Aeronautics and Astronautics in 1998. His research interests are structural dynamics and control.